Dedicated to Academician Aureliu Sandulescu's 80^{th} Anniversary

ISOTOPIC DEPENDENCE OF THE PRODUCTION CROSS SECTIONS OF SUPERHEAVY NUCLEI

G. G. ADAMIAN[1], N. V. ANTONENKO[2], W. SCHEID[3]

[1]Joint Institute for Nuclear Research, 141980 Dubna, Russia
Email: adamian@theor.jinr.ru
[2]Joint Institute for Nuclear Research, 141980 Dubna, Russia
Email: antonenk@theor.jinr.ru
[3]Institut für Theoretische Physik der Universität, 35392 Giessen, Germany
Email: werner.scheid@theo.physik.uni-giessen.de

Received August 4, 2011

Here, we consider various details of the calculation of evaporation residue cross sections for the production of superheavy elements, as the potential energy surface and the fusion rate. As example we present evaporation residue cross sections for the cold fusion reactions Zn + ^{208}Pb and the hot fusion reactions ^{48}Ca + ^{A}Cm and discuss their isotopic dependence.

Key words: Superheavy elements, mechanism of fusion, isotopic dependence of evaporation cross section.

PACS: 25.70.-z, 25.70.Jj, 27.90.+b.

1. INTRODUCTION

Already in the year 1975 Sandulescu [1], using the fragmentation theory [2], predicted suitable target and projectile nuclei for the production of superheavy nuclei. He suggested to choose the partners of a reaction with respect to the minima in the driving potential, calculated as a function of the mass- and charge asymmetry coordinates. This theory was supported by experiments done in Dubna at the same time to the element $Z = 104$ with the ^{50}Ti + ^{208}Pb reaction and to the element $Z = 106$ with the ^{54}Cr + ^{206}Pb reaction.

Superheavy elements are produced in fusion reactions with the emission of a few neutrons. One discriminates between cold fusion which are reactions like

$$^{70}\mathrm{Zn} + ^{208}\mathrm{Pb} \rightarrow ^{277}\mathrm{Cn} + \mathrm{n}$$

with the emission of a single neutron, and hot fusion reactions as

$$^{48}\mathrm{Ca} + ^{238}\mathrm{U} \rightarrow ^{283}\mathrm{Cn} + 3\,\mathrm{n}.$$

In the later case the formed compound nucleus has a higher excitation energy of about 35 MeV. No unique description of the reaction mechanism can presently be found for the fusion to superheavy nuclei in the literature. One may distinguish an adiabatic

view which lets the projectile and target nuclei melt together, and a description [3,4] based on the nuclear molecular concept which is denoted as dinuclear system (DNS) model and which assumes the fusion as a nucleon or cluster transfer from the lighter cluster to the heavier one up to the point when the lighter cluster has vanished and the compound nucleus is formed. Since we are convinced after various calculations that the DNS model describes the fusion correctly, we will base this presentation on the DNS concept.

The fusion dynamics can be described by two principle coordinates besides other essential coordinates like the deformation parameters and the neck coordinate. These two main coordinates are the relative coordinate R between the nuclear centers and the mass asymmetry coordinate η defined as

$$\eta = (A_1 - A_2)/(A_1 + A_2), \tag{1}$$

where A_1 and A_2 are the mass numbers of the two clusters. The mass asymmetry coordinate η phenomenologically (collectively) describes the transfer of nucleons between the touching clusters. The evaporation residue cross section can be quite generally written as [5]

$$\begin{aligned} \sigma_{ER}(E_{c.m.}) &= \sum_J \sigma_{cap}(J, E_{c.m.}) P_{CN}(J, E_{c.m}) W_{sur}(J, E_{c.m.}) \\ &\approx \sigma_c(E_{c.m.}) P_{CN}(E_{c.m.}) W_{sur}(E_{c.m.}). \end{aligned} \tag{2}$$

Here, σ_{cap} is the capture cross section when the projectile has crossed the outer Coulomb barrier and the target and projectile nuclei have transferred their relative kinetic energy into intrinsic excitation energy of the system. They get caught into the minimum of the internuclear potential at about $R_m \approx R_1 + R_2 + 0.5$ fm, where R_1 and R_2 are the radii of the projectile and target, respectively. The capture cross section for the transition of the colliding nuclei over the entrance Coulomb barrier can be approximated by $\sigma_c = (\lambda^2/4\pi)(J_{max}+1)^2 T(E_{c.m.})$ with the transmission probability $T = 0.5$ and $J_{max} = 10$ (see below). After the capture the system keeps its internuclear coordinate at R_m and begins to transfer nucleons between the two clusters up to the moment that an excited compound nucleus is formed. During the transfer of nucleons quasifission processes can occur with large probabilities. The probability to reach the compound nucleus is P_{CN}. The excited compound nucleus looses his excitation energy by the emission of neutrons. The probability to end at the ground state of the superheavy nucleus is W_{sur}. The angular momenta in the evaporation residue cross section are restricted by the survival probability to $J_{max} \approx 10$ when highly fissile superheavy nuclei are formed at incident energies near the Coulomb barrier.

In Section 2 we discuss the potential energy surface, in Section 3 it is qualitatively shown how the barriers in the potential influence the cross sections of fusion

and quasifission where quasifission means the decay of the system before the compound nucleus is formed. In Section 4 we demonstrate the isotopic behavior of the evaporation residue cross sections for cold and hot fusion reactions. Finally, Section 5 gives our conclusions.

2. THE POTENTIAL ENERGY SURFACE

The potential energy surface (PES) in the DNS model gives information about the optimal projectile-target combination and influences the fusion probability significantly. The PES is defined as [5]

$$U(A_1,A_2) = B(A_1) + B(A_2) + V(R,A_1,A_2) - \left(B(A_{CN}) + V_{rot}^{CN}(J)\right), \quad (3)$$

$$V(R,A_1,A_2) = V_C(R,Z_1,Z_2) + V_N(R,A_1,A_2) + V_{rot}(J) \quad (4)$$

with $A_{CN} = A_1 + A_2$ the mass number of the compound nucleus. $B(A_i)$ $(i = 1,2)$ and $B(A_{CN})$ are the negative binding energies of the clusters $i = 1,2$ and compound nucleus, respectively. The potential energy surface is referred to the ground state band energy $B(A_{CN}) + V_{rot}^{CN}(J)$ of the compound nucleus rotating with the angular momentum quantum number J. The binding energies are taken as experimental data and include the shell effects and pairing energies. The potentials $V_C(R,Z_1,Z_2)$, $V_N(R,A_1,A_2)$ and $V_{rot}(J)$ are the Coulomb, nuclear and centrifugal parts of the nucleus-nucleus potential, respectively. The centrifugal potential $V_{rot} = \hbar^2 J(J+1)/(2\Im)$ depends on the moment of inertia $\Im$ of the DNS. Since the overlap between the clusters is about a few percent of the total DNS volume, the DNS moment of inertia at the sticking limit can be calculated in a simple manner as $\Im = \Im_1 + \Im_2 + \mu R^2$ where μ is the mass of the relative motion. The Coulomb interaction can be approximated with the expansion [6]

$$V_C(R,Z_1,Z_2) = \frac{Z_1 Z_2 e^2}{R} + \left(\frac{9}{20\pi}\right)^{1/2}\left(\frac{Z_1 Z_2 e^2}{R^3}\right)\sum_{i=1}^{2} R_i^2 \beta_i P_2(\cos\vartheta_i) + \left(\frac{3}{7\pi}\right)^{1/2}\left(\frac{Z_1 Z_2 e^2}{R^3}\right)\sum_{i=1}^{2} R_i^2 \left(\beta_i P_2(\cos\vartheta_i)\right)^2, \quad (5)$$

where R_i and β_i are the radius and quadrupole deformation of the ith nucleus, respectively. ϑ_i is the angle between the distance vector $\vec{R}$ and the symmetry axis of the ith nucleus. For the nuclear interaction potential we take a Skyrme-type interaction without a dependence on the momentum and spin. Further, the sudden approximation

is assumed. The nuclear potential is given as [7]

$$V_N(A_1,A_2)=C_0\left(\frac{F_{in}-F_{ex}}{\rho_0}\int\left(\rho_1^2(\vec{r})\rho_2(\vec{r}-\vec{R})+\rho_1(\vec{r})\rho_2^2(\vec{r}-\vec{R})\right)d^3\vec{r}\right.$$
$$\left.+F_{ex}\int\rho_1(\vec{r})\rho_2(\vec{r}-\vec{R})d^3\vec{r}\right) \quad (6)$$

with

$$F_{in(ex)}=f_{in(ex)}+f'_{in(ex)}\frac{N_1-Z_1}{A_1}\frac{N_2-Z_2}{A_2}. \quad (7)$$

$N_{1,2}$ and $Z_{1,2}$ are the neutron and proton numbers of the clusters, respectively. The chosen parameters are $C_0=300$ MeV·fm^3, $f_{in}=0.09$, $f_{ex}=-2.59$, $f'_{in}=0.42$ and $f'_{ex}=0.54$. These parameters were fitted and describe a large number of experimental data [8]. The densities of the heavy nuclei are represented by two-parameter symmetrized Woods-Saxon functions $\rho_i(\vec{r})=\rho_0\sinh(R_i/a_i)(\cosh(R_i/a_i)+\cosh(r/a_i))$ where $\rho_0=0.17$ fm^{-3} gives the density of the nuclei inside. The nuclear radius parameter is chosen as $r_0=1.15$ fm and the diffusion parameter $a_i=0.54$ fm for ^{48}Ca and $a_i=0.56$ fm for actinide targets. In figure 1 we present the internuclear poten-

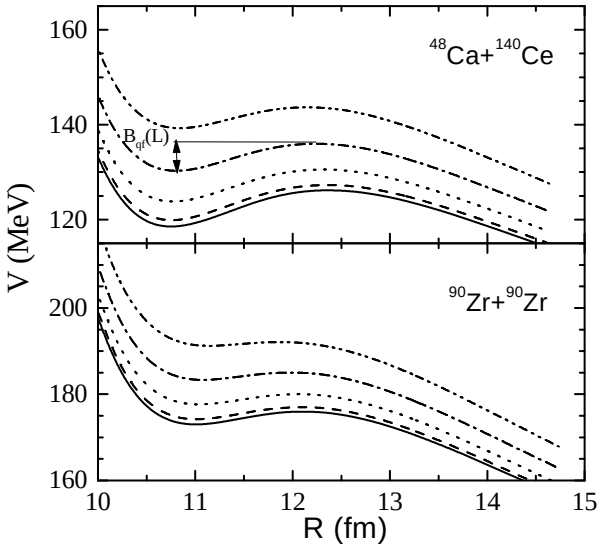

Fig. 1 – The figure shows the dependence of the internuclear potential on R and $L=J$ for the reactions ^{90}Zr + ^{90}Zr and ^{48}Ca + ^{140}Ce. The calculated results at $L=J=0$, 20, 40, 60 and 80 are given by solid, dashed, dotted, dash-dotted and dash-dotted-dotted curves, respectively. The quasifission barriers B_{qf} for the initial configurations depend on the angular quantum number and are about 7 - 6 MeV for the ^{48}Ca + ^{140}Ce reaction and 3 - 2 MeV for the ^{90}Zr + ^{90}Zr reaction.

tials for two cluster configurations. The curves show the characteristic behavior of potentials between clusters. From outside coming one first recognizes the Coulomb barrier and then the minimum where the cluster are in a touching position at $R = R_m$ and form the DNS. The difference between the Coulomb barrier and the minimum is the quasifission barrier indicated in figure 1. The potentials can also be calculated with the Strutinsky method using the liquid drop model and the two-center shell model. The result of the last method is very similar to the here applied procedure given by equation (3).

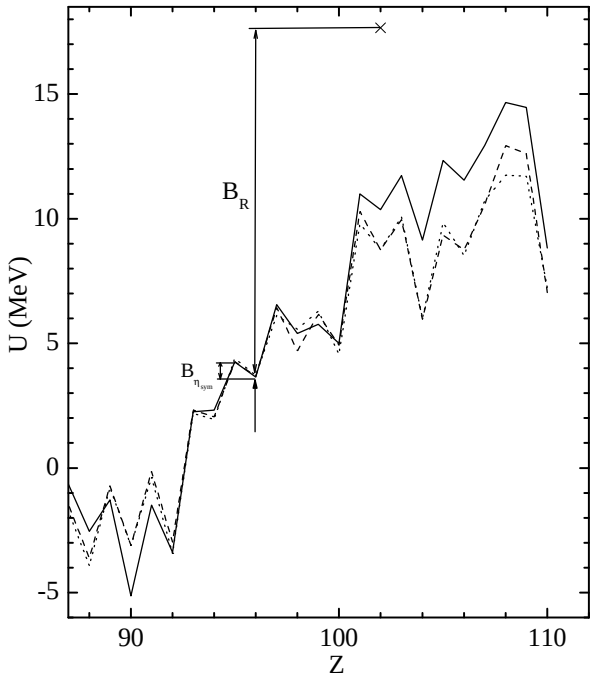

Fig. 2 – The DNS potential at the touching distance R_m of the clusters for $J = 0$ as a function of Z of the heavy nucleus , given by dotted, dashed and solid curves for the reactions ^{48}Ca + ^{244,246,248}Cm, respectively. The arrow points to the initial DNS. For the ^{48}Ca + ^{248}Cm reaction we show the barriers $B_{\eta_{sym}}$ ($Z_i = 96$, $N_i = 152$) and B_R ($Z = 102$, $N = 160$, $J = 0$) (see text). Here, Z and N are the charge and neutron numbers of the heavy nucleus, respectively. The potential energies are the energies above the energies of the corresponding compound nuclei. (Figure is taken from [10].)

3. DRIVING POTENTIAL AND PROBABILITY FOR COMPLETE FUSION

The probability of complete fusion P_{CN} can be analyzed within the transport theory. From the initial configuration on, there is a competition between complete

fusion in η, the diffusion in η to more symmetric DNS and quasifission. These processes can be described with a Kramers-type expression. The probability is [9]

$$P_{CN} = \lambda_{\eta}^{Kr} / \left(\lambda_{\eta}^{Kr} + \lambda_{\eta_{sym}}^{Kr} + \lambda_{R}^{Kr} \right) \tag{8}$$

and depends on the quasi stationary rates $\lambda_{\eta}^{Kr} = \lambda_{fus}^{Kr}$ for fusion, $\lambda_{\eta_{sym}}^{Kr}$ for symmetrization of the DNS, and λ_{R}^{Kr} for quasifission. The rates are functions of the various barriers in the driving potential measured form the minimum in the driving potential at η_i where the initial configuration is located. There is the fusion barrier B_{fus}^{*} in η, a barrier $B_{\eta_{sym}}$ in η in the direction to more symmetric configurations and the quasifission barrier B_{qf} in the relative coordinate R. The fusion rate is approximately given by

$$\lambda_{fus}^{Kr} \approx C_{fus} \exp\left(- \left(B_{fus}^{*} - \min(B_{\eta_{sym}}, B_{qf}) \right) / T \right). \tag{9}$$

The local temperature of the DNS is obtained from $T = \sqrt{E^{*}/a}$ where $a = (A_1 + A_2)/12$ MeV^{-1} and E^{*} is the excitation energy of the DNS. The constant C_{fus} depends on the frequencies of the inverted harmonic oscillators which approximate the internuclear potential in the coordinates R and η around the various barriers B_{fus}^{*}, B_{qf} and $B_{\eta_{sym}}$, and on friction coefficients.

In cold fusion, mainly quasifission arises from the initial DNS since the quasifission barrier B_{qf} is smaller than the barrier $B_{\eta_{sym}}$ to more symmetric configurations. However, in hot fusion reactions we have $B_{qf} > B_{\eta_{sym}}$. Then the DNS starts to proceed to symmetric systems and goes to quasifission in these configurations. In cold fusion reactions we calculate $B_{\eta_{sym}} \approx 4 - 5$ MeV whereas in hot fusion reactions this value is $B_{\eta_{sym}} \approx 0.5 - 1.5$ MeV. Therefore, hot fusion reactions have a decay of the DNS outside the initial minimum in contrast to the cold fusion reactions.

In figure 2 we show the driving potentials for $J = 0$ for the hot fusion reactions ^{48}Ca + ^{244,246,248}Cm as functions of the charge Z of the heavy nucleus. A minimization of the energy with respect to the N/Z ratio has been done for each value of Z. These isotopes have the largest yields. The potential energy decreases with the decrease of the total number of neutrons of the DNS and, therefore, we expect a larger primary yield for superheavy nuclei in the reactions of ^{244,246}Cm with ^{48}Ca which also results in our calculations [10]. Further in figure 2, there are depicted the barrier $B_{\eta_{sym}}$, which is quite small and does not much hinder the system to proceed to more symmetric clusters which decay by quasifission, and the barrier B_R. The initial configuration has a quasifission barrier of the order of $B_{qf} \approx 4$ MeV. The barrier B_R is defined as $B_R(Z, N, J) = U(R_b, Z, N, J) - U(R_m, Z_i, N_i, J)$ with $Z_i = 96$ and $N_i = 152$ (i is initial) where R_b means the radial position of the outside Coulomb barrier and Z and N are the charge and neutron numbers of the heavy nucleus, respectively. In figure 2 $B_R = B_R(Z = 102, N = 160, J = 0) \approx 14$ MeV is

shown.

4. ISOTOPIC EFFECTS IN THE PRODUCTION CROSS SECTIONS

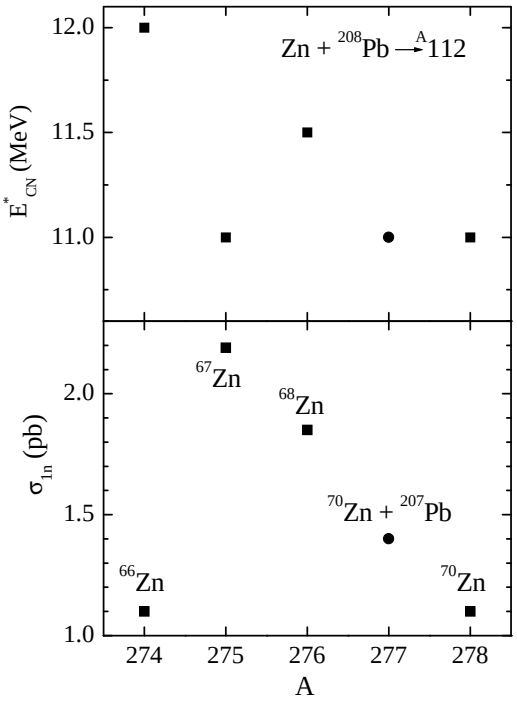

Fig. 3 – The calculated maximal evaporation residue cross sections in the $1n$ channel (lower part) at the corresponding excitation energies of the compound nuclei (upper part) for the fusion reactions Zn + ^{208}Pb $\rightarrow$ ^{A}Cn and ^{70}Zn + ^{207}Pb $\rightarrow$ ^{276}Cn as functions of A . The projectiles are indicated. (Figure is taken from [11].)

The isotopic behavior of σ_{ER} is essentially dependent on the product $P_{CN}W_{sur}$ of the fusion and survival probabilities. In the interval of A considered in figure 3 the value of P_{CN} strongly decreases with increasing A. Also the survival probability W_{sur} slightly increases with the decreasing mass number from $A = 278$ to $A = 274$ due to a large level spacing at $N = 162$ for deformed nuclei [11]. The larger P_{1n}, the probability of realization of the $1n$ channel, and the larger fission barrier and smaller neutron binding energy lead to a larger W_{sur} for the odd nucleus ^{275}Cn in comparison to its neighboring even-even nuclei (see figure 3). The considered reactions shown in figure 3 start from a minimum in the corresponding driving potential because of the magic ^{208}Pb target nucleus.

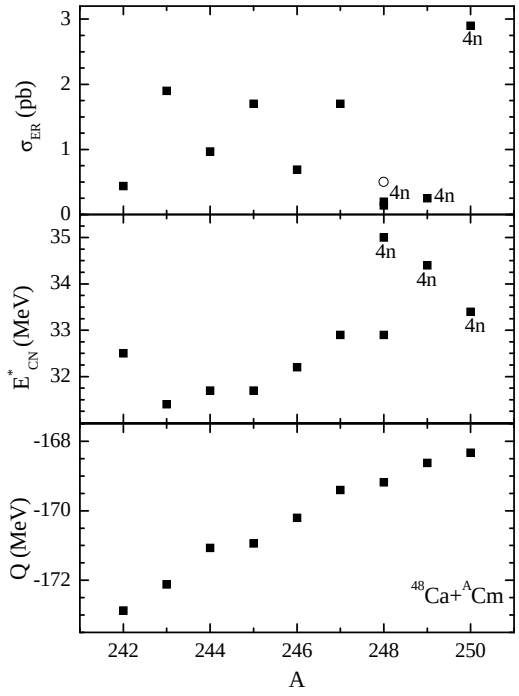

Fig. 4 – The maximal evaporation residue cross sections in the $3n$ channel (upper part) at the corresponding excitation energies of the compound nuclei (middle part) and Q values (lower part) for the fusion reactions ^{48}Ca + ^{A}Cm as functions of the mass number A of the target. Also maximal evaporation residue cross sections in the $4n$ channel (upper part) at the corresponding excitation energies of the compound nuclei (middle part) are given. The experimental data of the reaction ^{48}Ca + ^{248}Cm $\rightarrow$ ^{292}116 + $4n$ ($E^*_{CN} \approx 31 - 36$ MeV) [12] are shown by an open circle. (Figure is taken from [9].)

Calculated evaporation residue cross sections at the maxima of the excitation functions, the corresponding excitation energies of the compound nuclei in the $3n$ and $4n$ evaporation channels and the Q values are shown in figure 4 for the reactions ^{48}Ca + ^{A}Cm. The value of P_{CN} again increases with a decreasing value of A in most cases. The Q values, the excitation energy E^*_{CN} and the survival probability W_{sur} increase with A in the considered interval. Larger values of the realization probability P_{3n} and larger fission barriers, and smaller neutron binding energies give larger W_{sur} for the odd-even nuclei such as ^{243,245,247}Cm compared with those of the neighboring even-even nuclei (see figure 4).

The available data [12] can be well described. We estimate an inaccuracy of our calculations of σ_{ER} within a factor of 2–4. Already an inaccuracy in the value of B^*_{fus} creates an inaccuracy within a factor of 2. Since we did the calculations for all reactions with the same parameters and assumptions, the accuracy of the isotopic

dependence (or relative values of cross sections) is quite high.

Our calculations show larger cross sections, within a few picobarns, in the actinide-based reactions with a ^{48}Ca projectile and the target nuclei ^{229}Th, ^{235,236}U, $^{240-242}$Pu and ^{243,245,247,250}Cm. In hot fusion-evaporation reactions actinide targets with a smaller neutron excess are more effective in certain intervals than those with a larger neutron excess.

5. CONCLUSIONS

From the presented calculations we can learn and understand that not only the minimum in the driving potential is decisive for the production of superheavy nuclei as thought in the early times of these studies, but also that the heights of the barriers around the minimum, which essentially determine the fusion and quasifission rates, and in addition the survival probabilities are very important. All these quantities depend on shell and deformation effects. In addition the deformation and the orientation of the nuclear axes have to be considered as dynamical degrees of freedom (static behavior included in the above results). The calculations can be used in practice for the selection of suitable projectile and target combinations and optimal incident energies leading to maximum evaporation residue cross sections.

REFERENCES

1. A. Sandulescu, R. K. Gupta, W. Scheid, W. Greiner, Phys. Lett. **60B**, 225 (1976).
2. H. J. Fink, J. Maruhn, W. Scheid, W. Greiner, Z. Phys. **268**, 321 (1974).
3. V. V. Volkov, Izv. AN SSSR ser. fiz. **50**,1879 (1986).
4. V. V. Volkov, "*Deep Inelastic Nuclear Reactions*" (Energoizdat Moskow, 1982).
5. G. G. Adamian, N. V. Antonenko, W. Scheid, V. V. Volkov, Nucl. Phys. A **633**, 409–420 (1998).
6. N. Wang, J. Q. Li, E. G. Zhao, Phys. Rev. C **78**, 054607 (2008).
7. G. G. Adamian, N. V. Antonenko, N. Nenoff, W. Scheid, Phys. Rev. C **64**, 014306 (2001).
8. A. B. Migdal, "*Theory of Finite Fermi Systems and Application to Atomic Nuclei*" (Nauka Moskowa, 1982).
9. G. G. Adamian, N. V. Antonenko, W. Scheid, Phys. Rev. C **69**, 014607 (2004).
10. G. G. Adamian, N. V. Antonenko, A. S. Zubov, Phys. Rev. C **71**, 034603 (2005).
11. G. G. Adamian, N. V. Antonenko, W. Scheid, Phys. Rev. C **69**, 011601(R) (2004).
12. Yu. Ts. Oganessian *et al.*, Eur. Phys. J. A **13**, 135 (2002); **15**, 201 (2002).